# Closed-loop approaches to control of a wake flow modeled by the Ginzburg–Landau equation

**Article** *in* Computers & Fluids · August 2005

DOI: 10.1016/j.compfluid.2004.08.001



Available online at www.sciencedirect.com
SCIENCE DIRECT®
Computers & Fluids 34 (2005) 927–949
computers & fluids
www.elsevier.com/locate/compfluid

# Closed-loop approaches to control of a wake flow modeled by the Ginzburg–Landau equation

Kelly Cohen [a], Stefan Siegel [a,*], Thomas McLaughlin [a], Eric Gillies [b], James Myatt [c]

[a] *Department of Aeronautics, US Air Force Academy, 2354 Fairchild, Dr. Suite 6H27, CO 80840-62222, United States*
[b] *Department of Aerospace Engineering, University of Glasgow, Glasgow, Scotland G12 8QQ, United Kingdom*
[c] *Air Force Research Laboratory/Air Vehicles Directorate, Wright-Patterson AFB, OH 45433, United States*

Received 13 August 2003; received in revised form 6 March 2004; accepted 8 August 2004
Available online 21 November 2004

**Abstract**

A short computational program was undertaken to evaluate the effectiveness of a closed-loop control strategy for the stabilization of an unstable bluff-body flow. In this effort, the non-linear one-dimensional Ginzburg–Landau wake model at 20% above the critical Reynolds number was studied. The numerical model, which is a non-linear partial differential equation with complex coefficients, was solved using the FEMLAB®/MATLAB® software packages and validated by comparison with published literature. At first, a model independent approach was attempted for wake suppression using feedback control. The closed-loop system was controlled using a conventional proportional-integral-derivative (PID) controller as well as a non-linear fuzzy controller. A single sensor is used for feedback, and the actuator is represented by altering the boundary conditions of the cylinder. Simulation results indicate that for a single sensor scheme, the increase in the sophistication of the control results in significantly shorter settling times. However, there is only a marginal improvement concerning the suppression of the wake at higher Reynolds numbers. The feedback control design was then augmented by switching over to a model-dependent controller. Based on computationally generated data obtained from solving the unforced wake, a low-dimensional model of the wake was developed and evaluated. The low-dimensional model of the unforced Ginzburg–Landau equation captures more than 99.8% of the kinetic energy using just two modes. Two sensors, placed in

* Corresponding author. Tel.: +1 719 333 9080; fax: +1 719 333 4813.
*E-mail address:* stefan.siegel@usafa.af.mil (S. Siegel).


doi:10.1016/j.compfluid.2004.08.001

the absolutely unstable region of the wake, are used for real-time estimation of the first two modes. The estimator was developed using the linear stochastic estimation scheme. Finally, the loop is closed using a PID controller that provides the command input to the variable boundary conditions of the model. This method is relatively simple and easy to implement in a real-time scenario. The control approach, applied to the 300 node FEMLAB® model at 20% above the unforced critical Reynolds number stabilizes the entire wake. Compared to the model-independent controllers, the controller based on the low-dimensional model is far more effective in the suppression of the wake at higher Reynolds numbers. Furthermore, while the latter approach employs only the estimated temporal amplitude of the first mode of the imaginary part of the amplitude, all higher modes are stabilized. This suggests that the higher order modes are caused by a secondary instability that is suppressed once the primary instability is controlled.


**Nomenclature**

| | |
|---|---|
| $A(x,t)$ | complex amplitude of the Ginzburg–Landau model |
| $C_{ij}$ | coefficients of the linear stochastic estimator |
| $c_n$, $c_d$ | complex coefficients of the Ginzburg–Landau model |
| $F(x,t)$ | external forcing in the Ginzburg–Landau model |
| $f_a$ | external forcing used in the low-dimensional POD model |
| $F_{fuzzy}$ | control input of fuzzy logic controller |
| $F_{PID}$ | control input of PID controller |
| $G_s(t)$ | time-varying gains |
| $g_k$ | is a quadratic non-linear function of the time-dependent mode coefficients |
| $K_P$ | proportional gain of the controller |
| $N(t)$ | noise parameter in the Ginzburg–Landau model |
| $Re$ | Reynolds number |
| $U$ | advection speed |
| $x$ | spatial coordinate |
| $z_i$ | temporal mode amplitude of POD model |
| $\delta$ | Dirac delta function |
| $\mu(x)$ | wake growth rate parameter |
| $\mu_{crit}$ | value of the wake growth parameter, at which the self-excited oscillations begin |
| $\mu_0$ | analogue of wake Reynolds number. Also referred to in text as "Reynolds number" |

## 1. Introduction

The phenomenon of vortex shedding behind bluff bodies has been a subject of extensive research. Many flows of engineering interest produce the phenomenon of vortex shedding and the associated periodic lift and drag response. Applications include aircraft and missile aerodynamics, marine structures, underwater acoustics, and civil and wind engineering. The ability to suppress the flow oscillations in the wake of a bluff body could be used to reduce drag, vortex induced vibrations and aerodynamic noise. Flows with absolute instabilities behind bluff bodies, an archetype of which is the cylinder wake, demonstrate self-excited oscillations even when all sources of noise are removed [1].

In a two-dimensional cylinder wake, self-excited oscillations in the form of periodic shedding of vortices are observed above a critical Reynolds number of around 50 [2]. This behavior is referred to as the von Kármán vortex street [3], where flow-induced non-linear oscillations lead to undesirable effects associated with unsteady pressures such as fluid–structure interactions due to lift/drag fluctuations [3]. This problem is of practical importance because, particularly at higher Reynolds numbers, vortex shedding is associated with strong periodic transverse forces that can damage structures [3]. Also, the wake vortices greatly increase the drag of a bluff body, compared to the steady wake that can be observed at lower Reynolds numbers (*Re*). Monkewitz [4] showed that the von Kármán vortex street is the result of an absolute, global instability in the near wake of the bluff body. Further downstream the flow turns convectively unstable.

For these detrimental reasons many attempts to improve the unsteady vortex street have been made. When active open loop forcing of the wake is employed, the vortices in the wake can be "locked" at the forcing signal. This also strengthens the vortices and consequently increases the drag. The cylinder wake may be controlled by forcing the flow. Open loop forcing has been successfully employed to delay boundary layer transition [1]. However, Gillies [1] argues that the control of global flow oscillations that are the result of absolute instability is more cumbersome. An effective way of suppressing the self-excited flow oscillations, without making changes to the geometry, is by the incorporation of active closed-loop flow control [1].

A closed-loop flow control system is comprised of an actuator (or set of actuators) that introduces a perturbation into the flow, to obtain desired performance. Furthermore, the controller acts upon information provided by a set of sensors. The basic closed-loop control strategies are the model independent approach, the optimal/suboptimal control approach and the low-dimensional approach.

*Model independent approach*: This involves the introduction of sensors in the wake and a control law (usually linear) which produces a command to the actuator that forces the flow. The advantages of this approach [3] are:

- No model of the flow field is required for controller design;
- Direct feedback eliminates the need for a state estimator;
- A simple control law may be implemented in an experimental set up with relative ease.

Experimental studies show that a linear proportional feedback control based on a single sensor feedback is able to delay the onset of the wake instability, rendering the wake stable at *Re* about 20% higher than the unforced case. Above $Re = 60$, a single-sensor feedback may suppress the original mode but destabilizes one of the other modes [3]. This approach is relatively simple to implement experimentally. However, the results are of limited use for the challenging problem of an absolutely unstable wake.

*Optimal/suboptimal control approach*: This approach is more structured as it applies conventional and proven model-based control strategies such as optimal control theory for flow control problems. The central idea here is to minimize a cost function that satisfies the Navier Stokes equations that govern the flow. For example, Abergel and Temam [5] developed conditions for optimality which minimizes a cost function that represents the drag on a body. The main disadvantage of the optimal control approach is the computational problems associated with the non-linearities of the cumbersome unsteady Navier Stokes-equations. To illustrate this issue, Li et al. [6] point out that for a steady-state problem that has $N$ time steps, the dimension of the unsteady problem is $N$ times larger in comparison. This drawback adversely effects real time implementation of optimal flow control and has led to the development of several sub-optimal approaches surveyed by Li et al. [6].

*Low-dimensional approach*: Low-dimensional modeling is a vital building block when it comes to realizing a structured model-based closed-loop strategy for flow control. For control purposes, a practical procedure is needed to break down the velocity field, governed by Navier Stokes partial differential equations, by separating space and time. A common method used to substantially reduce the order of the model is proper orthogonal decomposition (POD) [7]. This method is an optimal approach in that it will capture a larger amount of the flow energy in the fewest modes of any decomposition of the flow. The POD method may be used to identify the characteristic features, or modes, of a cylinder wake as demonstrated by Gillies [1].

The Ginzburg–Landau (G–L) model is frequently used in the literature for wake control studies and has been shown to allow semi-qualitative predictions of the bluff body wake with feedback [8–11]. In particular, the complex G–L equation, with suitable coefficients, models the salient stability/instability features of more geometrically complex bluff-body wakes [5,8]. An attractive characteristic of the G–L model is that it is relatively straightforward to integrate numerically, making it an effective tool for investigating prototypes of control strategies.

Cylinder wake flows, represented by the G–L model, are dominated by the dynamics of a relatively small number of characteristic large-scale spatial structures, as observed in experimental results for periodically forced vortex streets. The G–L model is a set of complex, non-linear partial differential equations using numerical finite element or difference schemes. A control model based on these equations is therefore not feasible for real time estimation and control. A desirable controller will on the one hand simply measure and control a *finite number of large-scale spatial structures*. On the other hand, it will keep the number of modes of the wake flow *low* by not exciting it into a higher dimensional state, such as aperiodicity and turbulence for example.

The main approach used by some of the previous feedback flow control research efforts [8–11], for control of the complex G–L equation, involves the employment of simple proportional control with the gains selected ad hoc based on physical insight. Lauga and Bewley [12,13] introduce a more rigorous approach based on linear robust control theory. A single sensor/actuator is used to develop an H-infinity controller using the linearized G–L equations as a design model. The controller provides effective results when applied to the non-linear G–L equation, which serve as a truth model, for Reynolds number of 100 [13]. Furthermore, it was shown that the developed method can stabilize the present system at *any* Reynolds number with a single actuator/sensor configuration if sufficiently high numerical precision is used in the control derivation [12]. However, in a more recent publication [14], the above authors noted that due to the diminishing controllability and observability of the open-loop unstable modes as the Reynolds number is increased, this theoretical result may not be useful in practice.

In this computational effort, the loss of observability associated with an increase in Reynolds numbers is circumvented using multiple sensors in the wake. This approach has been successfully demonstrated by Gillies [9,10] for the complex G–L equation. In addition, two different approaches for control of the complex Ginzburg Landau equation are compared to existing proportional control approaches to the wake flow control problem using the complex non-linear G–L equation.

The first approach is model independent and consists of direct feedback of sensor measurement to a controller. The gains of the controller are then designed using ad hoc methods. Three different closed-loop control laws for the Ginzburg–Landau equation are developed using the model-independent approach: (a) simple proportional gain based on the approach adopted by Park et al. [11] and Gillies [9], (b) proportional-integral-derivative (PID) control and (c) fuzzy logic variable gain techniques. The main objective of the controller is to extend the value of the analogue of critical wake Reynolds number as much as possible utilizing a single sensor. The analogue of critical wake Reynolds number, referred to in this paper as the Reynolds number, is the value at which unsteady vortex shedding begins.

The other basic approach utilized in this paper is model dependent, using a controller based on a reduced order model. If the complex spatio-temporal information is characterized by a relatively small number of quantities, then feedback may be computationally feasible. Therefore, to obtain a controller that can be implemented, a reduced-order model is sought to represent the characteristic features of the flow field. A common method used to reduce the model-order is proper orthogonal decomposition, commonly known as POD. The POD method may be used to identify the characteristic features, or modes, of a cylinder wake as demonstrated by Gillies [1]. This method is an optimal approach in that it will capture a larger amount of the flow energy with fewer modes than any other decomposition of the flow. Low-dimensional modeling, based on POD techniques, is a vital building block when it comes to realizing a structured model-based closed-loop strategy for flow control. The major building blocks of this structured approach are composed of a reduced order POD model, a state estimator and a controller. A truth model, based on numerical techniques, is required for computational simulations to verify the effectiveness of the developed approach. Finally, wind/water tunnel experimentation would be required for experimental demonstration.

In his investigations of active control schemes for stabilizing the Ginzburg–Landau wake, Gillies [9,10] showed that a proportional control strategy using a single sensor can successfully control the flow at no more than 5% above criticality. However, a proportional controller based on two sensors extends the envelope to 12.5% above criticality. The same qualitative behavior has been demonstrated in the 2D cylinder wake at low Reynolds numbers: here, the wake is controllable with a single sensor only up to a Reynolds number of around 80. At this point, Gillies suggested that more sensors be introduced for feedback purposes for a further extension of the criticality envelope. In this effort, a low-dimensional POD model is sought to control the wake of the Ginzburg–Landau model studied by Gillies [9,10] and Park et al. [11]. The introduction of a POD model provides a more effective method of controlling the Ginzburg–Landau wake based on two sensors. The paper is organized as follows: The next section describes the research objective and uniqueness of the developed approach. The Ginzburg–Landau equation is presented in the following section and the FEMLAB® [13] model is described subsequently. Then, model independent controllers are developed followed by the development of the estimation and controller schemes based on a reduced order model. A comparison of the results between the closed-loop simulations to that in literature is made in the penultimate section, and the conclusions to date of this research effort are summarized in final section.

## 2. Research objective

Recent research on closed-loop control of the Ginzburg–Landau model using a simple proportional fixed gain approach includes work by Park et al. [11], Roussopoulos and Monkewitz [8] and Gillies [9,10]. The closed-loop results, obtained using the proportional fixed gain method based on feedback from one or two sensors, provide only limited improvement concerning the extension of the 'vortex shedding' criticality. Gillies [10] recommended the introduction of multiple sensors for a further extension of criticality.

The main objective of this research effort is to develop an effective estimation and control scheme for closed-loop suppression of the Ginzburg–Landau model of the von Kármán vortex street. The developed strategy would aim at extending criticality without necessarily having to increase the number of sensors above two. Furthermore, the estimator would be designed to adapt to changes in Reynolds number for a fixed set of sensor number and placement. A secondary objective of this paper is to compare the effectiveness of a model-based controller to model independent approaches.

## 3. The Ginzburg–Landau wake model

The 1D Ginzburg–Landau (GL) equation chosen is based on Park et al. [11] and Gillies [9] as follows:

$$\frac{\partial A}{\partial t} + U\frac{\partial A}{\partial x} = \mu(x)A + (1 + \mathrm{j}c_\mathrm{d})\frac{\partial^2 A}{\partial x^2} - (1 + \mathrm{j}c_\mathrm{n})|A|^2 A + F(x,t) \tag{1}$$

where $A(x,t)$ is the complex amplitude and $U$, $c_\mathrm{d}$, $c_\mathrm{n}$ and $\mu(x)$ are real. $F(x,t)$ incorporates the effects of feedback actuation and noise. It is pertinent, here, to clarify the analogy between the low Reynolds number cylinder wake and the computational model used in this paper, which is based on the Ginzburg–Landau wake prototype. The wake of a circular cylinder or other bluff body at low Reynolds number is characterized by an absolutely unstable region in the near wake, which admits a temporally growing *global mode* that acts as a 'wavemaker' for the downstream wake oscillations. This absolutely unstable near wake makes the flow *globally unstable* and corresponds, approximately, to the vortex formation region. Downstream, the growth rate of the global mode diminishes and becomes negative and the flow becomes convectively unstable. Here, the flow acts as an amplifier for the intrinsic fluid oscillations in the near wake and the flow saturates to the familiar Kármán vortex street. The G–L wake, although one dimensional, has qualitatively similar features and has therefore been used in several control studies of wake flows in response to feedback. The G–L wake also admits temporally growing global modes and their growth rate varies linearly in the downstream direction according to $\mu(x) = \mu_0 + \mu' x$. With suitable parameter values, the G–L equation exhibits an absolutely unstable 'near wake' between the bluff body boundary condition $x = 0$ and the downstream position where

$$x = \frac{1}{\mu'}\left[\frac{U^2}{4(1 + c_\mathrm{d}^2)} - \mu_0\right] \tag{2}$$

This is an analogue to the near wake of a bluff body, and this region acts like an oscillator. It is this region that contains the globally unstable modes that must be suppressed by any oscillation suppression control scheme. These global modes should not be confused with POD modes, discussed later. Further downstream, the G–L wake becomes convectively unstable and amplifies the near wake oscillations. The dynamics of the flow are characterized by an emergent self-excited unstable response followed by a limit cycle (see Fig. 1) where growth in oscillation ends.

The G–L model used in this effort corresponds to the low Reynolds number, laminar, low-dimensional cylinder wake (the regular range persists up to $Re \sim 194$ as detailed by Williamson [15]). Beyond this range the nature of the vortex shedding transitions to several three dimensional regimes with increase in the Reynolds number [15]. When active open-loop forcing of the wake is employed, the vortices in the wake can be "locked" at the forcing signal. This also strengthens the vortices and consequently increases the drag. The cylinder wake may be controlled by forcing the flow. Open-loop forcing has been successfully employed to delay boundary layer transition [1]. He et al. [16] apply this open-loop forcing approach to the boundary control by rotation of the flow around a cylinder and show up to 60% drag reduction for Reynolds numbers of 200–1000. As opposed to that open-loop approach, in this effort, the unsteady wake is controlled using a feedback controller.

For the flow around cylinders, several forcing techniques affect the behavior of the flow; however, the wake response to forcing is similar for each, whether translation of the cylinder in the direction parallel to or perpendicular to the mean flow, rotation of the cylinder or alternate blowing and suction at the separation points [9]. Controlled forcing of the wake will be introduced into the G–L equation by an actuation function placed in the near wake, namely $F(x,t)$, using simple

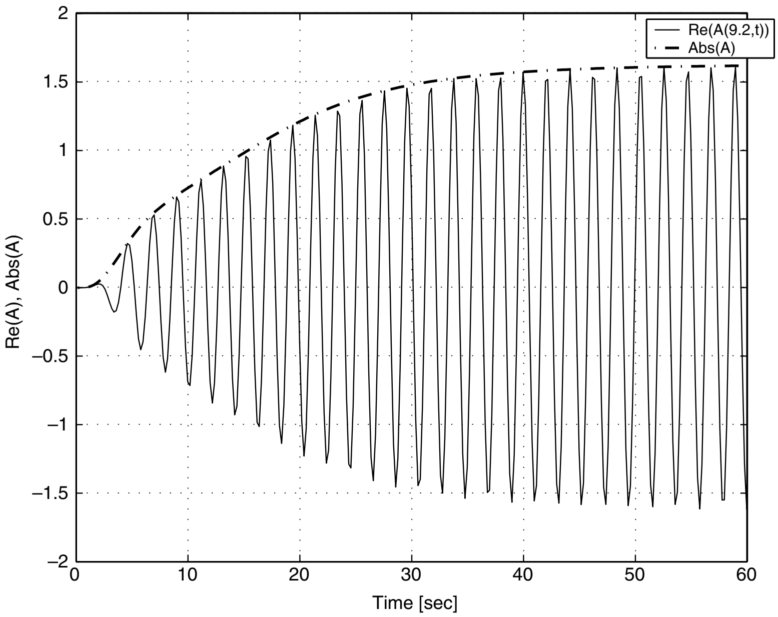


Fig. 1. Temporal plot of real part (solid line) and modulus (dot-dashed line) of $A(9.2,t)$ at 5% above $\mu_{\text{crit}}$.

delta functions with respect to the spatial variable $x$. The actuator will provide a step perturbation to the complex amplitude over the spatial actuation range: $0 < x_a < 2.0$.

The effects of feedback and noise may be incorporated into the GL equation in two ways. The first method, suggested by Roussopoulos and Monkewitz [8] and Gillies [9], involves modeling of the actuator as a delta function that provides forcing at a fixed spatial location, $x_a$, and a delta function that provides sensing at a sensor location, $x_s$, as shown in Eq. (3):

$$F(x,t) = \sum_{s=1}^{n} [G_s(t)A(x_s,t)] \cdot [\delta(x - x_a)] + N(t)\delta(x - x_a) \tag{3}$$

In the first term on the right of Eq. (3), signals from $n$ sensors are fed back with time-varying gains $G_s(t)$. The second term, $N(t)$, describes the noise added to the system. Noise may be modeled with a random number generator of adjustable amplitude. An alternative method for incorporating feedback and noise, utilized in this study, was proposed by Park et al. [11]. This approach involves the modeling of an active boundary condition at $x = 0$ for the Ginzburg–Landau equation as follows:

$$A(0,t) = \alpha(t)A(x_s,t) \tag{4}$$

where $\alpha(t)$ may be time-invariant as in the case of Park et al. [11] and Gillies [9] or it may be a variable gain. The current effort is based on Park et al. [11] and Gillies' [9] models to enable comparison:

- 1D domain $0 < x < 120$;
- Boundary conditions: $A(0,t) = 0$ (this simulates the cylinder body), $A(120,t) = 0$;
- Fixed parameters: $U = 5$; $\mu' = -0.0434$; $c_d = 1$; $c_n = 0$.

## 4. Computational model

After writing the GL equation, which is a non-linear partial differential equation with complex coefficients, the next step is to solve it numerically. After a survey of the market for an appropriate solver, FEMLAB®, developed by COMSOL [17], was selected. FEMLAB® is an interactive environment for finite-element modeling and simulating scientific and engineering problems based on partial differential equations (PDEs). FEMLAB's® ability to arbitrarily define and couple any number of non-linear PDEs, as well as work within the MATLAB®/SIMULINK® environment, makes it an attractive tool for studying fluid-control interaction. Furthermore, the solution of the Ginzburg–Landau equation is provided by FEMLAB® as a benchmark in their model library [17]. The size of the finite element model was determined by trial and error and 300 elements provide a fairly accurate model. The feedback forcing is introduced into the model by perturbing the boundary conditions at $x = 0$.

The details of the FEMLAB® model of the Ginzburg–Landau equation are as follows:

- *Element type*: 'solid1($x$)'—creates a 1-D solid object that spans all the coordinate values in the vector $x$ (1-D domain $0 < x < 120$).
- *Number of elements*: 300.

- *Number of nodes*: 301.
- *Boundary conditions*: $A(0,t) = 0$; $A(120,t) = 0$.
- *Time-step*: 0.2 units.
- *Total run-time*: 60 units.
- *Initial condition*: $A(x,0) = 0.0001$.

Gillies [9] reported that his wake model exhibits self-excited wake oscillations above $\mu_0 = \mu_{crit} = 3.43$. Theoretically, the GL wake, for the above coefficients, becomes globally unstable at $\mu_0 = \mu_{crit} = 3.438$. The above coefficients for the study of the spatially developing flows, based on the Ginzburg–Landau model, were first introduced by Park et al. [11]. The value of $\mu_{crit}$ is of importance; therefore an important step for validating the current work was to arrive at the same value of $\mu_{crit}$ using the model currently developed (using FEMLAB®) as Gillies [9]. Simulation results show that the FEMLAB® model predicts the value of $\mu_{crit}$ to within 0.3% of the theoretical value. Fig. 1 displays the temporal plot of the real part of $A(x,t)$ at 5% above criticality. Initially, the amplitude of the real part of $A(x,t)$ grows exponentially, and then it almost equilibrates at a saturated level, or limit cycle, due to the stabilizing cubic non-linearity. Furthermore, the FEMLAB® results shown in Fig. 1 compare well with those presented by Gillies [9]. Following the successful modeling of the open-loop behavior of the Ginzburg–Landau equation using FEMLAB®, the model may be exported to SIMULINK® for closed-loop studies. In this effort, two conditions are examined for the closed-loop studies, namely, 12.5% above $\mu_{crit}$ and 20% above $\mu_{crit}$.

## 5. Model independent approach

The uncertainties resulting from modeling errors inherent with wake flow dynamics and the effects of various disturbances make *robustness* an essential attribute of the control system. In order to circumvent many of the modeling and control problems mentioned, an estimator/controller strategy based on inherently robust soft computing techniques such as fuzzy logic was selected. The main advantages of using a fuzzy approach are the relative ease and simplicity of implementation and its robustness. The gains of the fuzzy controller may be adapted to provide fairly fast control for large deviations of the measured state of the plant from the desired state and a minor amount of control for small deviations.

The successful implementation of a fuzzy logic controller depends, among other design aspects, on the heuristic rule base from which control actions are derived. In order to obtain the required heuristic physics-based insight, a single degree of freedom system based on optimal control theory was analytically examined to observe the characteristics of a minimum time solution. Based on this analysis, Cohen et al. [18] introduced a fuzzy logic non-linear mapping function which has the potential of being a universal approximator to emulate the above minimum time solution. The resulting rule base is the core of the control law that is applied to the control of the Ginzburg–Landau equation presented herein. This approach has proved to be an effective means of controlling second-order systems by introducing a variable damping strategy which is implemented in the form of a fuzzy logic algorithm [19].

In the current effort, the fuzzy controller is described as follows:

$$F_{\text{fuzzy}} = \alpha_{\text{F}}(t) \cdot F_{\text{PID}} \tag{5}$$

where

$$F_{\mathrm{PID}} = -K_{\mathrm{P}}A(x_s,t) - K_{\mathrm{I}}\int_0^t A(x_s,t)\,\mathrm{d}t - K_{\mathrm{D}}\frac{\mathrm{d}(A(x_s,t))}{\mathrm{d}t} \tag{6}$$

is the conventional PID controller and $\alpha_{\mathrm{F}}(t)$ is the gain varying parameter that is the output of the fuzzy algorithm. The gains of the above PID controller ($K_{\mathrm{P}}$, $K_{\mathrm{I}}$ and $K_{\mathrm{D}}$) may be varied in real-time to provide fairly fast control for large deviations of the measured state of the plant from the desired state and a minor amount of control for small deviations. This adaptation strategy is implemented using fuzzy logic control and is based on successful implementation of a class of linear second-order systems [18]. The fuzzy controller is implemented as a 25-rule Mamdani fuzzy system with 2 inputs and 1 output as described by Cohen et al. [19].

The two inputs into the fuzzy algorithm are,

$$A(x_s,t), \frac{\mathrm{d}(A(x_s,t))}{\mathrm{d}t}$$

The single output from the fuzzy algorithm is $\alpha_{\mathrm{F}}(t)$.

Five membership functions are used to describe each of the input and output parameters. The respective membership functions for the input/output parameters are obtained after a tuning process. The Rule-Base is comprised of a set of 25 rules. Further details concerning the design of the fuzzy logic controller may be found in [18,19].

In order to examine the effectiveness of the variable gain strategy based on fuzzy logic control, results are compared to those obtained from the fixed gain controllers in the literature as well as the developed PID controller. The PID controller is the special case when $\alpha_{\mathrm{F}}(t) = 1$. The values of the gains of the PID controller are: $K_{\mathrm{P}} = 0.09$, $K_{\mathrm{I}} = 0.0$, and $K_{\mathrm{D}} = 0.06$.

## 6. Reduced order proper orthogonal decomposition modeling approach

Feasible real time estimation and control of the GL model may be effectively realized by reducing the model complexity using POD techniques. POD, a non-linear model reduction approach referred to in the literature as the Karhunen-Loeve expansion [7] is based on the spectral theory of compact, self-adjoint operators. The desired POD model contains an adequate number of modes to enable reasonable modeling of the temporal and spatial characteristics of the large-scale coherent structures inherent in the flow. Further details of the POD modeling may be found in Graham et al. [20,21]. A comprehensive treatise of the mathematical derivation of the POD method can be found in the book by Holmes et al. [7].

In this effort, the method of "snapshots" introduced by Sirovich [22] is employed to generate the basis functions of the POD spatial modes from the numerical solution of the GL equations obtained using FEMLAB®. The resulting spatial modes of the POD enable the GL equations to be projected using a least-squares method to yield a set of ordinary differential equations (ODE). After loading and arranging data obtained from the FEMLAB® solution of the GL wake model, the decomposition of $A(x,t)$ is as follows:

$$A(x,t) = A_{\mathrm{m}}(x) + A_{\mathrm{f}}(x,t) \tag{7}$$

where $A_{\mathrm{m}}$ (m/s) denotes the mean flow and $A_{\mathrm{f}}$ (m/s) is the fluctuating component that may be expanded as:

$$A_{\mathrm{f}}(x,t) = \sum_{k=1}^{n} a_k(t)\phi_i^{(k)}(x) \tag{8}$$

where $a_k(t)$ denotes the time-dependent coefficients having units of m/s and $\phi_i(x)$ represents the non-dimensional spatial eigenfunctions (see Figs. 2 and 3) determined from the POD procedure. From an ensemble of snapshots, the 'average snapshot' is computed and then this profile is subtracted from each member of the ensemble. This is done mainly for reasons of scale; i.e. the deviations from the mean contain information of interest but may be small compared with the original signal.

Next, the empirical correlation matrix, $R$ is computed. A simple approximation technique is applied to obtain the numerical integration. In this effort, the correlation matrix is computed using the inner product [7]. Solving the eigenvalue problem, the eigenvalues and the orthogonal spatial eigenfunctions, $\phi_i(x)$ are obtained. Since each eigenvalue measures the relative energy of the system dynamics contained in that particular mode, the eigenvalues may be normalized to correspond to a percentage. Finally, the time histories of the temporal coefficients of the POD model, $a_k(t)$, are determined using the extracted spatial modes and the data of the unforced flow. For an arbitrarily forced Ginzburg–Landau cylinder wake model, we can write the low-dimensional wake model as:

$$\frac{\mathrm{d}a_k}{\mathrm{d}t} = g_k(a_{\mathrm{n}}) + b_k f_{\mathrm{a}} \tag{9}$$

where $g_k$, for $k$ modes, is a quadratic non-linear function of the time-dependent mode coefficients. $b_k$ are coefficients associated with the control input, and $f_{\mathrm{a}}$ is the feedback control input to the

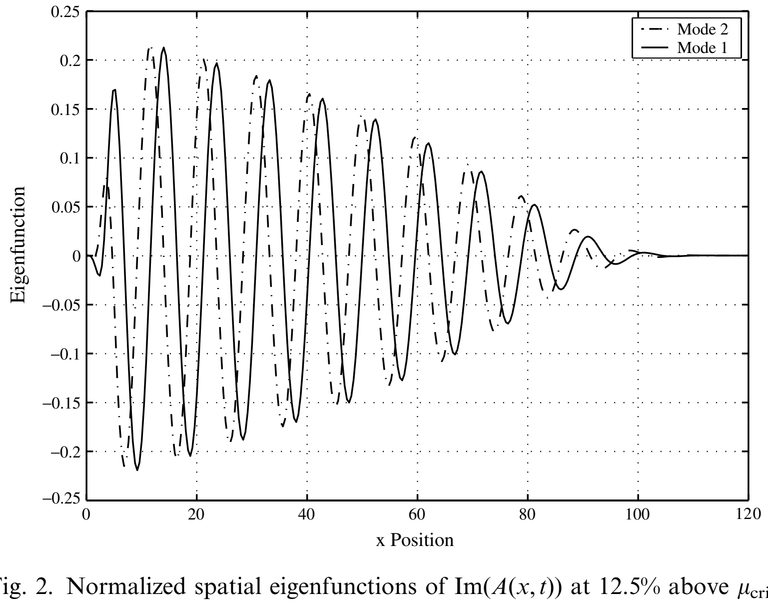


Fig. 2. Normalized spatial eigenfunctions of $\mathrm{Im}(A(x,t))$ at 12.5% above $\mu_{\mathrm{crit}}$.

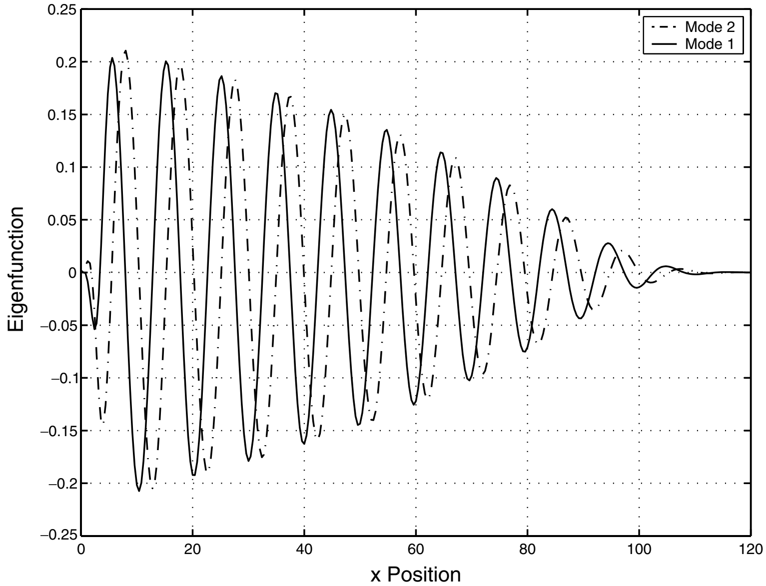


Fig. 3. Normalized spatial eigenfunctions of $\mathrm{Im}(A(x,t))$ at 20% above $\mu_{\mathrm{crit}}$.

cylinder. For the open-loop case $f_a = 0$. For a full state feedback system, the closed-loop control input, $f_a$, is a function of $a_k$. However, it is not possible to obtain a direct measurement of $a_k$. The POD algorithms, based on the above steps and realized in MATLAB®, were applied to the FEMLAB® data. The energy content for the first four modes is presented in Table 1. It can be seen that most of the kinetic energy of the flow lies in the first two modes. An important aspect of reduced order modeling is truncation. How many modes are important and what are the criteria for effective truncation?

The answers to the above questions were addressed by Cohen et al. [23]. Further details of the general, two-dimensional, bluff body wake control methodology may be found in Cohen et al. [24] (Fig. 4). This effort showed that control of the POD model of the von Kármán vortex street in the wake of a circular cylinder at $Re = 100$ is enabled using just the first mode. Furthermore, feedback based on the first mode alone suppressed all the other modes in the four mode POD model. At this point, it is imperative to note the difference between the number of modes required to *reconstruct* the flow and the number of modes required for effective low-dimensional modeling for control design. In this effort, we are interested in estimating only those modes required for closed-loop con-

Table 1
Energy content for the first four modes of the POD model

| Condition studied | Mode I | | Mode II | | Mode III | | Mode IV | |
|---|---|---|---|---|---|---|---|---|
| | Re (%) | Im (%) | Re (%) | Im (%) | Re (%) | Im (%) | Re (%) | Im (%) |
| 12.5% Above critical | 50.868 | 50.716 | 49.015 | 49.168 | 0.063 | 0.063 | 0.054 | 0.053 |
| 20.0% Above critical | 50.150 | 50.149 | 49.848 | 49.849 | 0.001 | 0.001 | 0.001 | 0.001 |

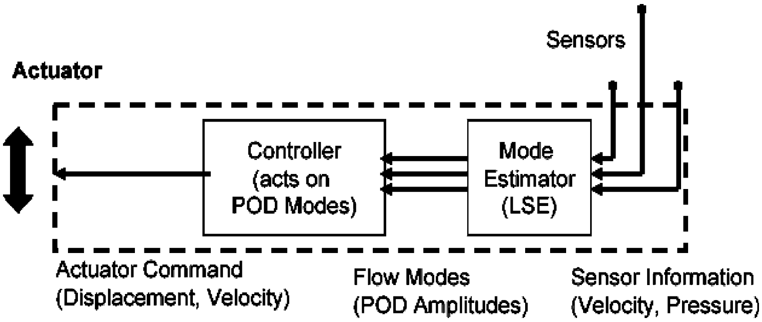


Fig. 4. Generic low-dimensional control strategy.

trol. On the other hand, an accurate reconstruction of the velocity field based on a low-dimensional model may be obtained using between 2 and 4 modes.

The POD algorithms, based on the above steps and realized in MATLAB®, were applied to the two conditions studied, namely, 12.5% above $\mu_{crit}$ and 20% above $\mu_{crit}$. The energy content for the first four modes of the real and the imaginary parts of $A(x,t)$ is presented in Table 1. It can be seen that more than 99.8% of the kinetic energy of the flow lies in the first two modes. It will be shown later that the estimation process is based on the $\mathrm{Im}(A(x,t))$ alone. The mode shapes for the first two modes for $\mathrm{Im}(A(x,t))$ are presented in Figs. 2 and 3 for both the conditions described in Table 1.

A close look at Figs. 2 and 3 shows the effect of increasing "Reynolds Number" on the mode shapes. As we move from 12.5% above $\mu_{crit}$ (Fig. 2) to 20% above $\mu_{crit}$ (Fig. 3), we observe that there is an increase in the value of the normalized eigenfunctions in the range between $0 < x < 10$. This is within the "absolutely unstable" region. The multiple sensor strategy examined by Gillies [9] comprised of placing two sensors: one at $x_1 = 4.8$ and the other at $x_2 = 9.6$. The signals received from these two sensors were utilized in the proportional feedback control law. This strategy enabled stabilizing the Ginzburg–Landau wake up to 12.5% above $\mu_{crit}$.

The estimation scheme developed in the next section takes the variations of the amplitudes of the normalized eigenfunctions into account. Two sensors are located similarly as above, namely one at $x_1 = 4.8$ and the other at $x_2 \sim 9.6$ and an adaptive estimation strategy is developed to account for the changes in the mode shapes. In this effort, the $x$-axis grid allows positioning of the two sensors at $x_1 = 4.8$ (node 13 of the FEMLAB® model) and at $x_2 = 9.2$ (node 24 of the FEMLAB® model). The implications of this approach make sense. In a realistic application, the sensor locations are usually fixed. The gains of the estimator may adapt to the Reynolds number, calculated in real-time based on velocity/pressure measurements, by utilizing a look-up table (see Table 4).

The time histories of the temporal coefficients of the POD model are determined by applying the least squares technique to the spatial modes and the unforced flow. These time histories are presented in Figs. 5 and 6 for both the conditions described in Table 1. The general hypothesis of this research effort is that the controller should be based on estimates of not more than Modes 1 and 2. The motivation is that for practical applications it is desirable to reduce the information required for estimation to the minimum. The requirement for the estimation scheme then is to behave as a modal filter that has "combed out" the higher modes. The primary aim of this approach

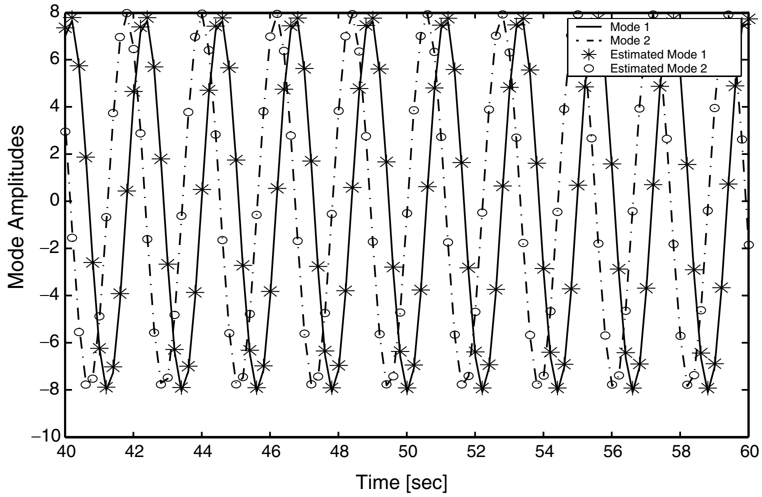


Fig. 5. Temporal mode amplitudes, $z_1$ and $z_2$, of $\mathrm{Im}(A(x,t))$ at 12.5% above $\mu_{\mathrm{crit}}$.

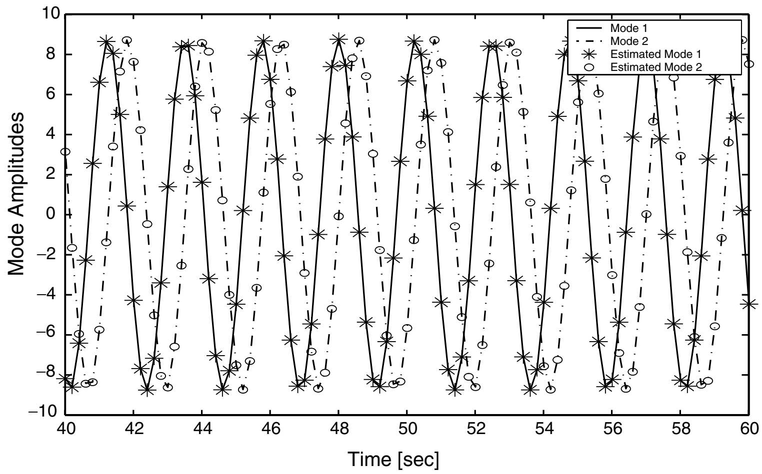


Fig. 6. Temporal mode amplitudes, $z_1$ and $z_2$, of $\mathrm{Im}(A(x,t))$ at 20% above $\mu_{\mathrm{crit}}$.

is to thereby circumvent the destabilizing effects of observation spillover as described by Balas [25]. Spillover has been the cause for instability in the control of flexible structures and modal filtering was found to be an effective remedy [26].

The intention of the proposed strategy is that the signals provided by the two sensors placed at $x_1 = 4.8$ and at $x_2 = 9.2$ are processed by the estimator to provide the estimates of the first two modes. The estimation scheme, based on the linear stochastic estimation procedure introduced by Adrian [27], predicts the temporal amplitudes of the first two POD modes from a finite set of measurements obtained from the uncontrolled solution of the Ginzburg–Landau wake model. Further details of stochastic estimation of POD modes are provided by Bonnet et al. [28].

Table 2
Coefficients $C_{ij}$ of the modal estimator

| Condition studied | $C_{11}$ | $C_{12}$ | $C_{21}$ | $C_{22}$ |
|---|---|---|---|---|
| 12.5% Above critical | 1.4524 | 4.1250 | 5.1486 | 4.1643 |
| 20.0% Above critical | 4.2744 | 6.9612 | 4.7633 | 0.1911 |

Recently, this method was also used by Carlson and Miller [29] to predict the degree of flow separation from POD modes on a backward facing ramp using ramp pressure measurements.

A set of 100 measurements at $x_1 = 4.8$ and at $x_2 = 9.2$ were extracted from the uncontrolled steady-state FEMLAB® solution. These measurements were at intervals of 0.2 s from $t = 40$ s until $t = 60$ s. The temporal mode amplitudes, $z_1$ and $z_2$, obtained in the previous section at the above 100 discrete times were mapped onto the extracted sensor signals, $\mathrm{Im}(A(x_1, t))$ and $\mathrm{Im}(A(x_2, t))$, as follows:

$$z_1(t) = C_{11} * \mathrm{Im}(A(x_1, t)) + C_{12} * \mathrm{Im}(A(x_2, t)) \tag{10}$$

$$z_2(t) = C_{21} * \mathrm{Im}(A(x_1, t)) + C_{22} * \mathrm{Im}(A(x_2, t)) \tag{11}$$

The coefficients $C_{ij}$ $(i,j = 1,2)$ in Eqs. (10) and (11) are obtained via the linear stochastic estimation method from the set of 100 discrete sensor signals and temporal mode amplitudes and are presented in Table 2. This procedure is performed just once for each Reynolds number before closing the feedback control loop. The main advantage of this approach is that it enables usage of sensors at fixed sensor locations with just the coefficients $C_{ij}$ adapting to the Reynolds number using the look-up table presented in Table 2. Basically, $C_{ij}$ represents the gains of the estimator, and the look-up table is the gain scheduler based on the modal estimation provided by Eqs. (10) and (11). Figs. 5 and 6 illustrate the effectiveness of the linear stochastic estimation process for the estimation of the first two temporal mode amplitudes $z_1$ and $z_2$.

## 7. Simulation, results and discussion

### 7.1. Model-independent approach

A linearization of the 300-node FEMLAB® model was exported to SIMULINK® for the closed-loop studies. The following parameters are defined:

- Settling time—Time taken until: $\mathrm{abs}[A(x_s, t)] \leqslant 0.05\max[A(x_s, t)]$.
- Sensor reading—$A(x_s, t)$ at $x_s = 3.2$ (Node 9).
- Parameter $\mu_{\mathrm{crit}}(P)$—Maximum value of $\mu_0$ that still provides stable closed-loop system for proportional control – $\mu_0 = 3.50$.

The time histories of $\mathrm{Re}(A(10, t))$ and the respective control input for the PID controller at $\mu_0 = 3.578$ are presented in Cohen et al. [19]. It is interesting to note that the control input is stabilized based on a sensor reading at $x_s = 3.2$. However, the sensor signal placed at $x = 10.0$ indicates that the wake has not stabilized. The linearized wake is diverging and that suggests that a

Table 3
Comparison of results for PID controller and fuzzy controller

| | Stabilization above $\mu_{crit}(P)$ [%] | Control effort at $\mu_0 = 3.567$ | Settling time at $\mu_0 = 3.567$ [s] |
|---|---|---|---|
| PID control | 100 | 0.0040 | 600 |
| Fuzzy logic control | 125 | 0.0029 | 200 |

mere shifting around of the flow pattern occurs without suppression of the wake along the $x$-dimension as desired. For the same value of $\mu_0 = 3.578$, the entire wake is stabilized using the fuzzy logic controller [19]. Finally, the fuzzy logic controller becomes unstable at $\mu_0 = 3.585$. Table 3 compares the results obtained using a fuzzy controller to those obtained using PID control. These results may be summarized as follows:

*PID vs. proportional control*—The PID control delays the onset of vortex shedding at twice the improvement obtained using P control. The settling time compared to literature (Park et al. [11] using just proportional feedback), shows an improvement of an order of magnitude.

*Fuzzy vs. PID*—Using fuzzy control, the onset of vortex shedding is further delayed by another 25% when compared to PID control. The settling time for the stable condition near "Re Critical" for the fuzzy controller is a third in comparison. The overall control effort (integral of control input over time for the same maximum allowable actuation) used by the PID controller is 38% more than the fuzzy design.

The results using a model-independent approach indicate that for a single sensor scheme, the increase in the sophistication of the control results in significantly shorter settling times. However, there is only a marginal improvement concerning the suppression of the wake at higher "Reynolds numbers". It seems that the only way to improve this is to incorporate a multi-sensor strategy. This finding clearly substantiates the work done by Gillies [9,10]. In addition, the model independent approach used to solve the Ginzburg–Landau equations does not appear feasible for real time estimation and control because modern control techniques have difficulty in handling a non-linear system having 300 degrees of freedom. Furthermore, the pursuit of a low-dimensional model may result in a more effective closed-loop control strategy. Wake flows, represented by the Ginzburg–Landau model, are dominated by the dynamics of a relatively small number of characteristic large-scale spatial structures, as observed in experimental results for a forced vortex street. A desirable controller will on the one hand simply measure and control a *finite number of large-scale spatial structures*. On the other hand, it will keep the complexity of the wake flow *low* by not exciting it into a higher dimensional state. If the complex spatio-temporal information is characterized by a relatively small number of quantities, then feedback can be computationally feasible. Therefore, to obtain a controller that can be implemented, a reduced-order model is sought to represent the characteristic features of the flow field.

### 7.2. Reduced order, POD based approach

The closed-loop system, realized in MATLAB®/SIMULINK®, is presented in Fig. 7. The FEMLAB® subsystem contains the 300 node, non-linear Ginzburg–Landau model. The four signals out of FEMLAB® are as follows for 12.5% above $\mu_{crit}$: $y_1 = \mathrm{Re}(A(4.8, t))$ and $y_2 = \mathrm{Re}(A(9.6, t))$, which are used for purposes of observation alone, and $y_3 = \mathrm{Im}(A(4.8, t))$ and

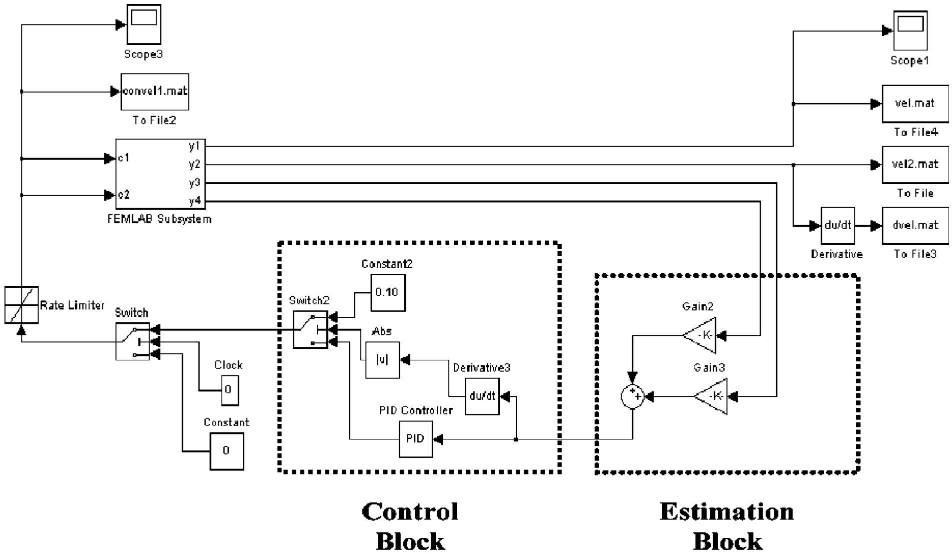


Fig. 7. SIMULINK© model of the closed-loop control system.

$y_4 = \mathrm{Im}(A(9.6, t))$, which are used for the estimation of the temporal mode amplitude. On the other hand, for 20% above $\mu_{crit}$: $y_1 = \mathrm{Re}(A(4.8, t))$, $y_2 = \mathrm{Re}(A(9.2, t))$, $y_3 = \mathrm{Im}(A(4.8, t))$ and $y_4 = \mathrm{Im}(A(9.2, t))$. Monitoring $y_1$ and $y_2$ as well ensures that the real part of the wake solution, $A(x, t)$, is stabilized (see Figs. 8 and 9). On the other hand, the best indicator that the imaginary part of the solution $A(x, t)$ is stabilized is by observing the control input (see Fig. 10). Although, we can provide estimates for both Modes 1 and 2 based on the sensor signals extracted from $x_1 = 4.8$ and $x_2 = 9.2$, it was found that for the two conditions studied, it is adequate for the controller to be based on the estimate of Mode 1 alone. In Fig. 7, Gains 2 and 3 in the Estimator

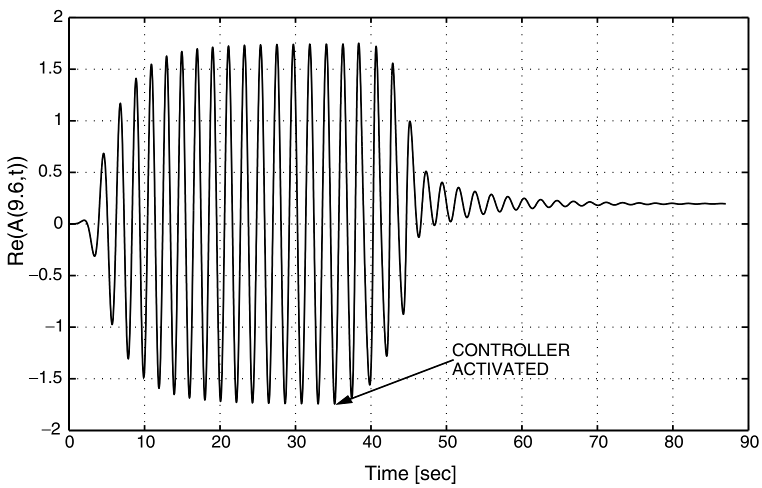


Fig. 8. Controlled wake signal at 12.5% above critical.

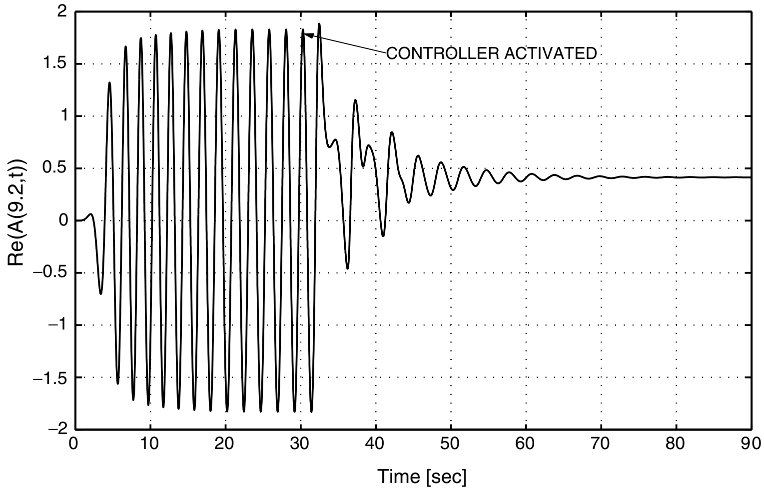


Fig. 9. Controlled wake signal at 20% above critical.

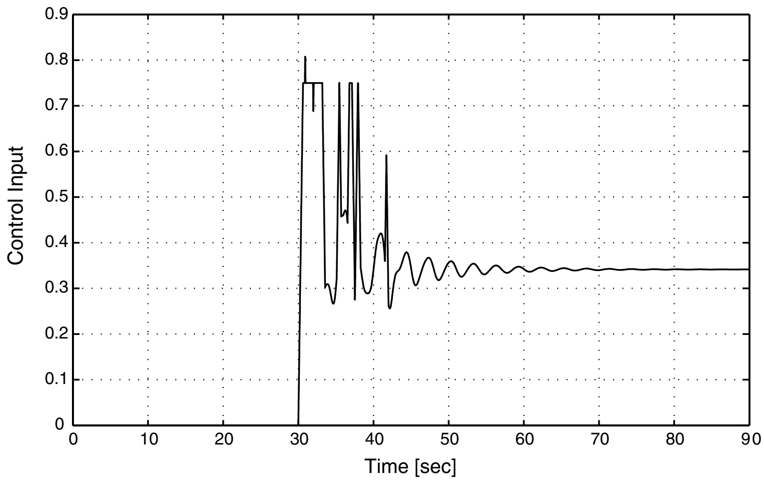


Fig. 10. Control input at 20% above critical.

Block correspond to coefficients $C_{11}$ and $C_{12}$ respectively. The input to the control block is just the estimate of Mode 1. The control scheme includes actuator saturation such that above a certain threshold for the derivative of estimated Mode 1, a constant control is applied. Below the threshold value a proportional-integral-derivative (PID) controller is applied. A proportional controller, with gain $K_P$, was found to be effective enough for the conditions studied, i.e. $K_D$ and $K_I$ were zero. The control law for POD based closed-loop system, as described in Eq. (9) is:

$$f_a = K_P z_1(t) \tag{12}$$

where $z_1(t)$ is the estimate of mode one described by Eq. (9). A rate limiter, with a slew rate of $\pm 1.2$, was introduced to ensure that only physical commands would be introduced by the control-

Table 4
Parameters of the controller for the two conditions studied

| Condition studied | $K_P$ | Constant control | Derivative threshold | Rate limiter slew rate | Controller switch-on time [s] |
|---|---|---|---|---|---|
| 12.5% Above critical | 0.017 | 0.10 | 5.0 | ±1.2 | 35 |
| 20.0% Above critical | 0.060 | 0.75 | 4.0 | ±1.2 | 30 |

ler into the FEMLAB subsystem. Finally, the control was activated arbitrarily after ensuring that the system had reached its limit cycle. The control parameters used for the two conditions studied are provided in Table 4, which is in fact a gain-scheduling look-up table that enables the controller to adapt to a varying Reynolds Number. The value of $K_P$ was obtained by tuning it in an ad hoc manner in non-linear simulations of the entire non-linear complex Ginzburg–Landau equation.

The results of the simulation are provided in Figs. 8–10. The estimation/control scheme developed in this effort provides effective stabilization of the Ginzburg–Landau wake at the two conditions studied. The non-linear dynamics of the Ginzburg–Landau model has a fixed point that is not at $A(x,t) = 0$, and the controller stabilizes the wake by converging to this fixed point (see Figs. 8 and 9). The control input time-history, shown in Fig. 10, illustrates the behavior of the controller for large values of the estimated derivative of Mode 1 ($25 < t < 40$). After 40 s, the PID controller takes over completely and stabilizes the system. The rate limiter ensures that the control command remains physically realizable in nature.

## 8. Global modes of the wake flow

Similar to a Navier–Stokes model of the wake behind a circular cylinder at low Reynolds number, it has been pointed out that the linearized form of the GL equation above admits a denumerable set of *global modes* (not to be confused with the POD modes used in the above control model). The growth rate of these global modes determines whether a point in the flow is locally absolutely unstable or locally convectively unstable. A further advantage of the GL equation for modeling flow control schemes for wake flows is that the growth rates and the global modes themselves are easily found. Each global mode is of the form

$$\phi_n(x)\exp(-j\omega_n t) \tag{13}$$

where the growth rate is found from the imaginary part of:

$$\omega_n = j(\mu_0 - (U^2/4(1 + jc_d)) + \{(1 + jc_d)\mu'^2\}^{1/3}\zeta_n) \tag{14}$$

The largest temporal growth rate is that of global mode 1. At higher values of this Reynolds number analogue, higher global modes become unstable, but, for uncontrolled flow, the most unstable global mode is dominant. If, by a single sensor feedback control, the first global mode is stabilized, then one of the other global modes oscillates unless it is controlled too, and so on. For the GL equation with our chosen values of coefficients the critical values at which the higher global modes become unstable are tabulated in Table 5.

It is the global modes themselves that become unstable and act as oscillators in the near wake, which saturate to the GL wake (or the Kármán vortex street in the cylinder flow); and hence it is

Table 5
Conditions for instability of the GL wake global modes

| Global mode | Critical $\mu_0$ | % Above $\mu_{crit}$ |
|---|---|---|
| One | 3.438 | 0.0 |
| Two | 3.672 | 6.8 |
| Three | 3.864 | 12.4 |
| Four | 4.034 | 17.3 |

the global modes themselves that have to be suppressed by any control strategy for suppression of flow oscillations. It is therefore interesting to note that, for a simple single sensor proportional feedback control (like Gillies [9]), the method fails approximately at the point where the second global mode becomes unstable; and the simple two sensor proportional control of Gillies [9] fails just at the point where the third global mode becomes unstable. It may be conjectured then that the number of sensors required for simple proportional feedback control is equivalent to the number of unstable global modes. It has to be stressed however, that the POD modes do not correspond to the global modes of the flow. The POD control strategy is more successful that the simple point sensor feedback—this must be because the POD modes encapsulate the dynamics of a number of global modes.

It might be thought that the global modes themselves, rather than sensor measurements or POD modes, would be efficient 'states' to be controlled within a control scheme. However, as in a true cylinder wake flow-where the global modes have only been observed fleetingly during the start of vortex shedding, the global modes only exist in the linear stages of wake oscillations. They grow exponentially and are quickly lost in the non-linear saturated wake state. The global modes themselves then, are not useful entities to observe within the controller. It is, however, the set of unstable, or destabilized, global modes that have to be stabilized by the controller if wake oscillations are to be suppressed.

That the single POD mode controller is able to suppress the wake oscillations at 20% above the critical Reynolds number, where there are four global modes, suggests that the POD modes are a more efficient representation of the global flow oscillations than the global modes.

## 9. Conclusions and recommendations

Although there is a vast literature on flow control, especially regarding the bluff body wake and the Ginzburg–Landau equation, there is relatively little of this literature which involves classical, or non-linear, control theory. Most (but not all) of the previous work has been concerned with ad hoc proportional control strategies applied to fluid problems, rather than studies involving detailed control theory. This work has aimed to redress this imbalance. A FEMLAB® model was developed to solve the Ginzburg–Landau equation that contains all the stability features of the 2-D cylinder wake pertinent to control. The developed model was exported to SIMULINK® for closed-loop studies. A gain-scheduling approach is proposed, whereby, for a given sensor configuration, the estimation and controller gains adapt by means of a look-up table to the variation in the Reynolds Number. This method is relatively simple and easy to implement in a real-time scenario. The control approach, applied to the 300 node FEMLAB® model at 20% above the unforced critical Reynolds number stabilizes the entire wake for a proportional gain of 0.06. While the controller uses only the estimated temporal amplitude of the first POD mode of $\mathrm{Im}(A(x,t))$, all higher POD modes are stabilized. This suggests that the higher order POD modes are slaved to the instability encapsulated by the first POD mode. Thus they are suppressed once the primary instability is controlled.

Simulation results show that using a model independent approach, a variable gain fuzzy logic control provided better response, compared to a fixed gain PID controller, with respect to the onset of vortex suppression, the settling times, as well as the control effort applied. However there is only a marginal improvement concerning the suppression of the wake at higher Reynolds numbers. On the other hand, it has been shown that by introducing an estimation scheme based on a low-dimensional POD model, two sensors are adequate for a substantial further extension of the onset of the instability from 12.5% above criticality to 20% above criticality. This successful stabilization of the Ginzburg Landau wake therefore used one POD mode at a Reynolds number where the flow has, in the linear sense, four unstable globally modes. The first POD mode must therefore encapsulate the dynamics of the first four global modes of the wake.

The successful control, which stabilized the GL wake at 20% above the critical Reynolds number, is seen to stabilize the wake about a different equilibrium to the mean flow during normal wake oscillations. This possibly has a consequence for cylinder wake control: traditionally the literature has attempted to use feedback control to stabilize the bluff body wake about the mean flow condition; whereas the current work suggests that other equilibrium conditions may be stabilized more successfully. It is difficult to conjecture, physically, what a non-zero stabilized equilibrium for the GL wake would correspond to in an actual bluff body wake. One possible condition, which *is* known to improve the stability of a bluff body wake, is a change in the symmetry of the flow (placing a small cylinder in the near wake (introducing a constant cylinder rotation is known to stabilize a wake flow to a small extent). Verification of this conjecture will require future study.

Continuing studies will aim at extending the onset of instability still further in an attempt to examine the limits of a two-sensor estimation/control strategy. In addition, the control approach will be further examined to observe its sensitivity to time delays, actuator limitations, modeling and estimation errors and sensor noise. In parallel, this approach will be applied to experimental and computational studies of the control of a two-dimensional circular cylinder wake at the US Air Force Academy.

The current work is analogous to control of the 2D wake of a circular cylinder between the Reynolds numbers of 40–50 (the onset of wake oscillations) and around 180 (the onset of three dimensionality). Prior to the onset of flow oscillations at the critical *Re*, the pressure drag of a circular cylinder is reducing; however in the laminar, periodic vortex shedding regime, the pressure drag starts to increase with further *Re*. This pressure drag has a periodic component, and is directly related to structure of the fluctuating vortex street in the wake. To reduce the drag we could either reduce the strength of the eddies or decrease the width of the wake: suppression of wake oscillation therefore directly influences the cylinder drag, and reduces the fluctuating drag component to zero. As we have used the 1D Ginzburg Landau model as a wake prototype, it is difficult to infer, directly, the effects of our controller on fluid dynamic drag. However, we have been completely successful in eliminating flow oscillations for the G–L wake 20% above the critical *Re*.

In simulations of control of the circular cylinder wake, Park et al. [30] showed that the drag at $Re = 60$ could be reduced from approximately 1.38 during wake oscillations to approximately 1.28 during control. Park et al. [30] also showed a reduction of drag coefficient from 1.34 during shedding at $Re = 80$ to approximately 1.28—even although wake oscillations were not completely suppressed by their controller at this higher $Re$.

Our controller sometimes stabilizes the flow at non-zero solutions to the Ginzburg–Landau equation. What this might mean, physically, for a wake flow is that our control strategy stabilizes a fixed, stationary vortex (or vortices) immediately behind the cylinder. This will mean that the fluctuating drag component can be reduced to zero, but that another drag component, resulting from this stationary vortex (or vortices) might be created. Future work, involving a full numerical solution of the 2D cylinder wake coupled to the controller, is required to investigate the effects of the controller on drag.

## Acknowledgments

The first author would like to acknowledge the support provided by the AFOSR/ESEP program. The authors would like to acknowledge the support and assistance provided by Dr. Belinda King and Lt. Col. Sharon Heise of the AFOSR.

## References

[1] Gillies EA. Low-dimensional control of the circular cylinder wake. J Fluid Mech 1998;371:157–78.
[2] Albarede P, Provansal M. Quasi-periodic cylinder wakes and the Ginzburg–Landau model. J Fluid Mech 1995;291:191–222.
[3] Roussopoulos K. Feedback control of vortex shedding at low Reynolds numbers. J Fluid Mech 1993;248:267–96.
[4] Monkewitz PA. Modeling of self-excited wake oscillations by amplitude equations. Exp Thermal Fluid Sci 1996;12:175–83.
[5] Abergel F, Temam R. On some control problems in fluid mechanics. Theor Comput Fluid Dyn 1990;1:303–25.
[6] Li Z, Navon IM, Hussaini MY, Le Dimet FX. Optimal control of cylinder wakes via suction and blowing. Comput Fluids 2003;32:149–71.
[7] Holmes P, Lumley JL, Berkooz G. Turbulence, Coherent Structures, Dynamical Systems and Symmetry. Cambridge, UK: Cambridge University Press; 1996.
[8] Roussopoulos K, Monkewitz PA. Nonlinear modeling of vortex shedding control in cylinder wakes. Physica D 1996;97:264–73.
[9] Gillies EA. Multiple sensor control of vortex shedding. In: Proceedings of 6th AIAA/CEAS Aeroacoustics Conference, Lahaina, Hawaii, 12–14 June 2000, AIAA Paper 2000-1933.
[10] Gillies EA. Multiple sensor control of vortex shedding. AIAA J 2001;39(4):748–50.
[11] Park DS, Ladd DM, Hendricks EW. Feedback control of a global mode in spatially developing flows. Phys Lett A 1993;182:244–8.
[12] Lauga E, Bewley T. The decay of stabilizability with Reynolds number in modes of spatially developing flows. Proc R Soc Lond A 2003;459:2077–95.
[13] Lauga E, Bewley T. Modern control of linear instability in a cylinder wake model. Int J Heat Fluid Flow 2002;23:671–7.
[14] Lauga E, Bewley TR. Performance of a linear robust control strategy on a nonlinear model of spatially-developing flows. J Fluid Mech 2004;512:343–74.

[15] Williamson CHK. Vortex dynamics in the cylinder wake. Annu Rev Fluid Mech 1996;28:477–539.
[16] He JW, Glowinski R, Metcalfe R, Nordlander A, Periaux J. Active control and drag optimization for flow past a circular cylinder. J Comp Phys 2000;163:83–117.
[17] FEMLAB, Version 2.2, COMSOL AB, November 2001.
[18] Cohen K, Weller T, Ben-Asher J. Control of linear second-order systems by a fuzzy logic based algorithm. J Guidance Control Dyn 2001;24(3):494–501.
[19] Cohen K, Siegel S, McLaughlin T, Myatt J. Fuzzy logic control of a circular cylinder vortex shedding model. In: Proceedings of 41st Aerospace Sciences Meeting and Exhibit, AIAA Paper 2003-1290.
[20] Graham WR, Peraire J, Tang KY. Optimal control of vortex shedding using low-dimensional models, Part I: Open-loop model development. Int J Numer Meth Eng 1999;44(7):945–72.
[21] Graham WR, Peraire J, Tang KY. Optimal control of vortex shedding using low-dimensional models, Part II: Model based control. Int J Numer Meth Eng 1999;44(7):973–90.
[22] Sirovich L. Turbulence and the Dynamics of Coherent Structures Part I: Coherent Structures. Quarter Appl Math 1987;45(3):561–71.
[23] Cohen K, Siegel S, McLaughlin T, Gillies E. Feedback control of a cylinder wake low-dimensional model. AIAA J 2003;41(7):1389–91.
[24] Cohen K, Siegel S, McLaughlin T. Control issues in reduced-order feedback flow control. In: Proceedings of 42nd Aerospace Sciences Meeting and Exhibit, AIAA Paper 2004-0575.
[25] Balas MJ. Active control of flexible systems. J Optim Theory Appl 1978;25(3):217–36.
[26] Meirovitch L. Dynamics and control of structures. New York: John Wiley & Sons, Inc.; 1990. p. 313–51.
[27] Adrian RJ. On the role of conditional averages in turbulence theory. In: Zakin J, Patterson G, editors. Proceedings of the Fourth Biennial Symposium on Turbulence in Liquids. Princeton: Science Press; 1977. p. 323–32.
[28] Bonnet JP, Cole DR, Delville J, Glauser MN, Ukeiley LS. Stochastic estimation and proper orthogonal decomposition: complementary techniques for identifying structure. Exp Fluids 1994;17:307–14.
[29] Carlson H, Miller R. Reduced-order modeling and sensing of flow separation on lifting surfaces. In: Proceedings of 40th AIAA Aerospace Sciences Meeting and Exhibit, Reno, Nevada, 14–17 January 2002, AIAA Paper 2002-0975.
[30] Park DS, Ladd DM, Hendricks EW. Feedback control of von Kármán vortex shedding behind a circular cylinder at low Reynolds numbers. Phys Fluids 1994;6(7):2390–405.